Janus Cages of Bilayered Polymer–Inorganic Composites

ARTICLE *in* MACROMOLECULES · MAY 2013

Impact Factor: 5.8 · DOI: 10.1021/ma4006236

Macromolecules

Article

pubs.acs.org/Macromolecules

Janus Cages of Bilayered Polymer–Inorganic Composites

Ying Chen, Haili Yang, Chengliang Zhang, Qian Wang, Xiaozhong Qu, Jiaoli Li, Fuxin Liang,* and Zhenzhong Yang*

State Key Laboratory of Polymer Physics and Chemistry, Institute of Chemistry, Chinese Academy of Sciences, Beijing 100190, China

Supporting Information

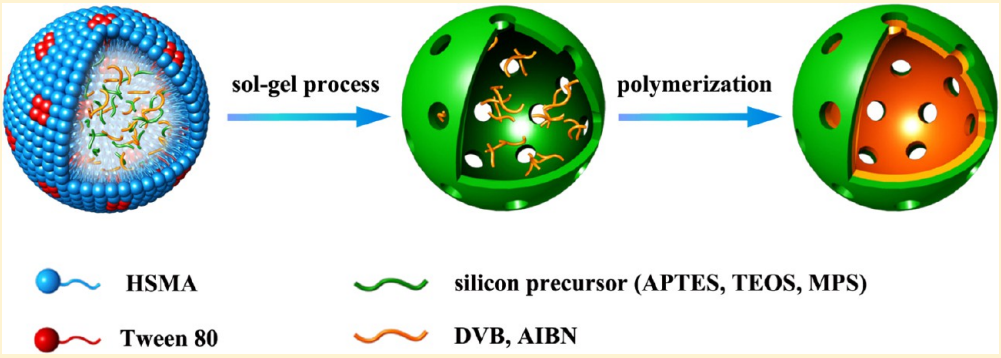

ABSTRACT: Janus cages with a bilayer polymer–inorganic composite shell are synthesized by an emulsion interfacial self-organized sol–gel process followed by a polymer grafting onto the interior surface containing a vinyl group. Binary surfactants experience a phase separation to create transverse channels across the shell. The Janus cages can be functionalized by either growing responsive polymers or integrating with functional nanoparticles. They are promising in controlled loading and triggered release of desired materials under guidance.

1. INTRODUCTION

Janus objects with two different compositions compartmentalized have gained growing academic and industrial interests due to their diversified performances.[1,2] Currently, those noncentrosymmetric Janus materials have been extensively reported with varied shapes including particle,[3] rod,[4] and disk.[5] Two different compositions are compartmentalized onto the same surface. Recently, centrosymmetric hollow spheres but with an asymmetric shell are becoming a key concern.[6] Such hollow spheres are recognized as Janus to mimic micellar structures. They can serve as specific containers, and desired compounds can be selectively captured thereby from their surroundings due to different affinity. The performance is promising in controlled loading and release and confined catalytic reaction.[7]

Organic Janus hollow spheres have been extensively synthesized based on either self-assembly from amphiphilic molecules or seed emulsion polymerization. Their shells are rather weak that are easily swollen and weakening in the presence of solvents even after they are strengthened by polymerization or cross-linking. In the absence of transverse channels, mass transportation through the shell is restricted.[7b] Robust inorganic shell is a rational alternative. Recently, we have reported a Janus silica hollow microsphere by an emulsion interfacial self-assembled sol–gel process, whose interior surface is hydrophobic and the exterior surface is hydrophilic.[6] One large window hole is resulted after dissolving the interior core, providing a window for hydrophobic materials being selectively captured inside the cavity from a hydrophilic environment.[6] However, the irregular window lacks of control in both shape and size. Moreover, the interior surface terminated with the pedant group from the silane lacks of responsive performance. It is required to create tunable transverse channels to enhance selective mass transfer forming Janus cages. It will be more interesting if the Janus cages are responsive.

Herein, we extend our previous interfacial materialization synthesis of inorganic Janus hollow spheres to large scale fabricate Janus porous hollow spheres with a bilayered polymer–inorganic composite shell as illustrated in Scheme 1. Self-organized sol–gel process of silicon precursors proceeds at the emulsion interface to form inorganic Janus cages first; polymer–inorganic composite Janus cages were achieved by subsequently grafting polymer onto the interior face of the inorganic Janus ones. It is key to employ binary surfactants to create transverse pores across the shell after a phase separation at the emulsion interface during the sol–gel process.[8] The interior polymeric layer gives a tunable hydrophobic cavity to selectively collect oil, while the hydrophilic silica exterior layer ensures a good dispersibility of the microspheres in water.

Received: March 26, 2013
Revised: April 30, 2013
Published: May 8, 2013

   dx.doi.org/10.1021/ma4006236 | *Macromolecules* 2013, 46, 4126–4130

Scheme 1. Schematic Synthesis of a Janus Cage with Bilayered Polymer−Inorganic Composites

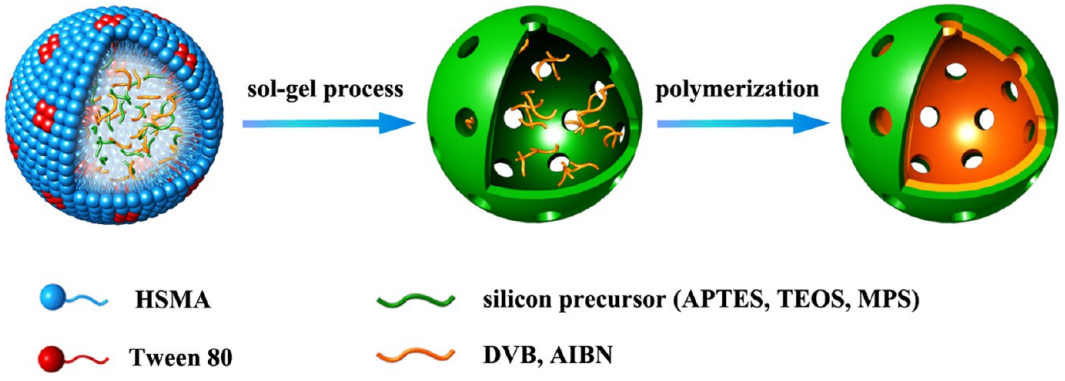

2. EXPERIMENTAL METHODS

2.1. Materials. 3-Methacryloxypropyltrimethoxysilane (MPS), γ-aminopropyltrimethoxysilane (APTMS), and γ-aminopropyltriethoxysilane (APTES) were purchased from Alfa Aesar. Tween-80, azodiisobutyronitrile (AIBN), *n*-decane, toluene, tetraethyl orthosilicate (TEOS), sodium oleate, iron chloride ($FeCl_3$), and oleic acid were purchased from Sinopharm Chemical Reagent Beijing Co., Ltd. 1,1′-Dioctadecyl-3,3,3′,3′-tetramethylindocarbocyanine perchlorate (dil-C18) and divinylbenzene (DVB) were purchased from Sigma-Aldrich. Hydrolyzed styrene−maleic anhydride (HSMA) copolymer was synthesized.[9] DVB was purified over Al_2O_3 column. *N*-Isopropylacrylamide (NIPAM) was purchased from J&K Chemical and recrystallized with toluene and *n*-hexane. All other reagents were used as received without further purification.

2.2. Preparation of the Polymer−Inorganic Bilayered Composite Janus Cages. An example recipe is given as following. 15 mL of 10 wt % hydrolyzed styrene−maleic anhydride (HSMA) copolymer solution and 0.03 g of Tween-80 were dissolved in 75 mL of water. pH of the mixture was adjusted to 2.5 with 2 M aqueous hydrochloric acid. 10 g of *n*-decane, 1.1 g of APTES, 1.24 g of MPS, 5.2 g of TEOS, 10 g of DVB, and 0.1 g of AIBN were mixed. The oil mixture was dispersed into the aqueous solution after a homogenization at a speed of 12 000 rpm for 5 min, forming an oil-in-water emulsion. The emulsion was held under stirring at 25 °C for 7 h for the sol−gel process. Afterward, the emulsion was heated to 70 °C to initiate the polymerization for 12 h. Polymer−inorganic bilayered composite Janus cages were obtained.

2.3. Preparation of Oleic Acid-Modified Fe_3O_4 Nanoparticles.[10] Aqueous solutions of sodium oleate and iron chloride were mixed at an equal molar ratio to obtain iron oleate. The resultant brown iron oleate precipitate was then filtered, washed for three times with distilled water, and dried in a desiccator. Iron oleate (2 g) complex was added to a solution containing 20 mL of ethanol and 2 mL of oleic acid at room temperature. The resulting mixture was transferred into a Teflon-lined stainless steel autoclave with a capacity of 25 mL, heated to 180 °C, and kept for 5 h. The autoclave was cooled to room temperature naturally, and the product was collected at the bottom of the vessel. Paramagnetic oleic acid modified Fe_3O_4 nanoparticles about 10 nm were obtained.

2.4. Preparation of the Paramagnetic Janus Cages. An example recipe is given as following. 15 mL of 10 wt % hydrolyzed styrene−maleic anhydride (HSMA) copolymer solution and 0.03 g of Tween-80 were dissolved in 75 mL of water. The pH of the mixture was adjusted to 2.5 with 2 M aqueous hydrochloric acid. 10 g of *n*-decane, 1.1 g of APTES, 1.24 g of MPS, 5.2 g of TEOS, 10 g of DVB, 0.1 g of AIBN, and 0.3 g of oleic acid-modified Fe_3O_4 nanoparticle were mixed. The oil mixture was dispersed into the aqueous solution with a homogenizer at a speed of 12 000 rpm for 5 min, forming an oil-in-water emulsion. The emulsion was held under stirring at 25 °C for 7 h for the sol−gel process. Afterward, the emulsion was heated to 70 °C to initiate the polymerization for 12 h. Paramagnetic Janus cages were obtained.

2.5. Preparation of the Thermal Responsive Janus Cages. An example recipe is given as following. 10 mL of 10 wt % hydrolyzed styrene−maleic anhydride (HSMA) copolymer solution and 0.05 g of Tween-80 were dissolved in 75 mL of water. The pH of the mixture was adjusted to 2.5 with 2 M aqueous hydrochloric acid. 2.5 g of toluene, 0.6 g of APTMS, 0.8 g of MPS, and 3.0 g of TEOS were mixed. The oil mixture was dispersed into the aqueous solution with a homogenizer at a speed of 12 000 rpm for 2 min, forming an oil-in-water emulsion. The emulsion was held under mechanical stirring at 70 °C for 12 h. Inorganic Janus hollow cages were obtained.

0.02 g of sodium dodecyl sulfate (SDS) was dissolved in 4 g of water, while 1 g of *N*-isopropylacrylamide and 0.05 g of AIBN were dissolved in 1.5 g of toluene. Then the toluene phase was dispersed into the aqueous solution under vigorously stirring to form a stable emulsion. The emulsion was added into the inorganic Janus hollow cage dispersion in 5 g of water. The mixture was stirred with a magnetic stirrer in a nitrogen atmosphere to allow a favorable collection of NIPAM/AIBN/toluene inside the cavity and heated to 70 °C for 12 h to form a responsive Janus cage.

2.6. Characterization. Structure and morphology of the samples were characterized using transmission electron microscopy (JEOL 100CX operating at 100 kV) and scanning electron microscopy (Hitachi S-4800 at 15 kV) equipped with an energy dispersive X-ray (EDX) analyzer. The samples for SEM observation were prepared by vacuum sputtering with Pt after being ambient dried. The samples for TEM observation were prepared by spreading very dilute dispersions in ethanol onto carbon-coated copper grids. FT-IR spectroscopy measurement was performed after scanning samples for 32 times using a Bruker EQUINOX 55 spectrometer with the sample/KBr pressed pellets. Thermogravimetric analysis (TGA) was performed using the PerkinElmer Pyris 1 TGA under air at a heating rate of 10 °C/min. Particle size and distribution were measured by dynamic light scattering (DLS) using a Zetasizer (Nano Series, Malvern Instruments). Polarizing optical micrograph images were performed using Olympus optical microscope. Florescence microscopy images were observed using a confocal laser scanning microscope (CLSM, Leica TCS-sp2, Germany).

3. RESULTS AND DISCUSSION

First, an oil-in-water emulsion forms with hydrolyzed styrene−maleic anhydride (HSMA) copolymer and Tween-80 as surfactants. The oil phase is composed of *n*-decane, oil-soluble monomer divinylbenzene (DVB), initiator azodiisobutyronitrile (AIBN), and three silanes: 3-methacryloxypropyltrimethoxysilane (MPS), γ-aminopropyltriethoxysilane, and tetraethyl orthosilicate. The emulsion is kept for a sol−gel process at 25 °C for 7 h. Under acidic conditions, for example at pH of 2.5, the sol−gel process predominantly occurs at the emulsion interface to form a Janus porous silica layer.[6,11] The amine group and propenyl group are distinctly compartmentalized onto exterior and interior surfaces of the shell, respectively. The

dx.doi.org/10.1021/ma4006236 | Macromolecules 2013, 46, 4126−4130

emulsion is further heated to 70 °C to graft a polymer onto the propenyl- group-terminated interior surface. Since polydivinylbenzene (PDVB) is insoluble in *n*-decane, phase separation occurs at early polymerization stage forming PDVB clusters. The clusters remain active, which can be further covalently bound onto the polymeric layer. The interior polymer surface becomes coarsened. After dissolution of the internal oil phase, micrometer-sized polymer−inorganic bilayered composite Janus hollow spheres form (Figure 1a). The presence of

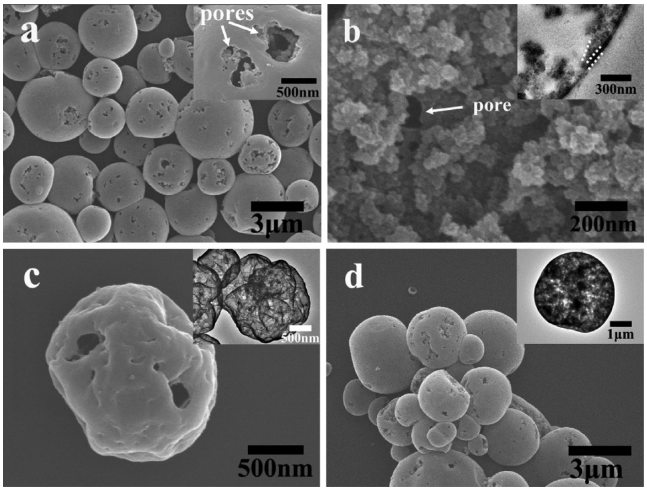

Figure 1. (a) SEM images of the Janus composite cage and inset magnified pores; 10 g of DVB is used. (b) SEM image of the interior side and inset cross-section TEM image of the Janus composite cage. (c) Silica cage derived from the composite Janus cage (a) after a selective removal of polymer by calcination at 450 °C in air. (d) PDVB cage derived from the composite Janus cage (a) after a selective removal of silica with 10 wt % aqueous HF.

PDVB and silica of the Janus composite cage is confirmed by FT-IR spectroscopy (Figure S1). The peak at 3020 cm^{-1} is the typical stretching vibration of the aromatic C−H bond. The absorption peak at 2926 cm^{-1} is attributed to the stretching vibration of CH_2. The peak centered at 1720 cm^{-1} is assigned to C═O of MPS. The peaks around 1600−1449 cm^{-1} correspond to the skeleton vibration of the benzene ring. The peak at 1096 cm^{-1} is assigned to the asymmetrical stretching vibration of Si−O−Si. The multiple absorption peaks between 900 and 708 cm^{-1} are associated with the C−H out-of-plane bending vibration. The peak at 3434 cm^{-1} reveals the presence of the amine group. The example Janus cage contains 6.5 wt % of silica measured by thermogravimetric analysis (TGA) in air (Figure S2). The average diameter is 3 μm (Figure S3) measured by dynamic light scattering (DLS). There exist transverse channels across the shell (inset Figure 1a). Observation of a broken hollow sphere indicates the interior surface is coarsened, and some transverse pores are visible (Figure 1b). Cross-section TEM image reveals the polymer/inorganic bilayered structure (inset Figure 1b). Further labeling with acidic-group-capped Au nanoparticles reveals that the amine group is exclusively distributed onto the exterior surface.[5b] In order to further confirm the bilayered structure, silica (Figure 1c) and PDVB (Figure 1d) cages are derived after selective removal of PDVB by calcination in air at 450 °C and silica by etching with 10 wt % aqueous HF, respectively.

The microstructure of the interior polymer layer is tunable. For instance, the interior surface becomes smooth and the thickness of the internal polymer layer becomes thinner with decreasing graft content (Figure 2a,b). When a hydrophobic

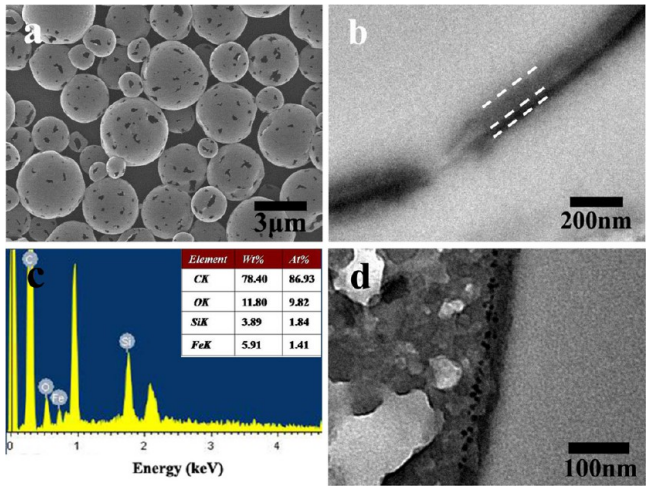

Figure 2. (a) SEM and (b) cross-section TEM images of the Janus composite cage; 5 g of DVB is used. (c) EDX spectrum of the paramagnetic Janus composite cage. (d) Cross-section TEM image of the paramagnetic Janus composite cage containing hydrophobic Fe_3O_4 nanoparticles.

oleic acid-capped Fe_3O_4 nanoparticle is previously introduced in the oil phase, a paramagnetic Janus composite cage is achieved (Figure S4). The Fe element is detected by energy dispersive X-ray (EDX) analysis (Figure 2c). The cross-section TEM image indicates that the nanoparticles are mainly sandwiched at the polymer/silica interface (Figure 2d).

Tween-80 is determinative to create the transverse pores across the shell, since Tween-80 can induce a phase separation with HSMA at the emulsion interface.[8] Tween-80 acts as a porogen to induce formation of the porous shell. If no Tween-80 is added in the aqueous phase, no pores form (Figure 3a). At low level of Tween-80 (0.03 wt %), channels are created (Figure 1a). At increasing content of Tween-80, for example

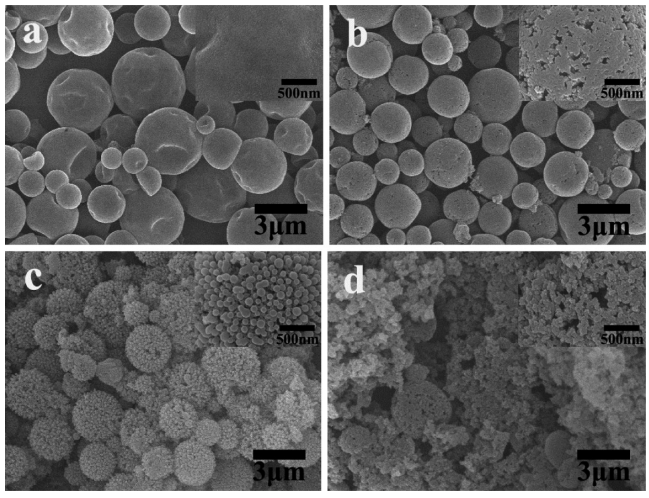

Figure 3. SEM images of the Janus composite cages synthesized at varied Tween-80 concentration in aqueous phase (wt %): (a) 0; (b) 0.22; (c) 0.44; (d) 0.67. DVB feeding amount is fixed at 10 g.

dx.doi.org/10.1021/ma4006236 | *Macromolecules* 2013, 46, 4126−4130

0.22 wt %, the shell becomes porous (Figure 3b). At higher content for example 0.44 wt %, the shell becomes locally discontinuous, and small silica particles appear on the exterior surface (Figure 3c). Their spherical contour is preserved. No change is found of the small particles after calcination in air at 450 °C (Figure S5a), which can be etched with 10 wt % aqueous HF (Figure S5b). More Tween-80 (0.67 wt %) causes disintegration of the spherical contour (Figure 3d).

The Janus composite cages can serve as unique containers to mimic micelles, but more robust, desired components can be selectively collected inside the cavity from their surroundings. Upon addition of the example Janus cage (Figure 1a) into the immiscible toluene–water mixture, toluene is preferentially captured inside the cage (Figure 4a). The saturation capacity is

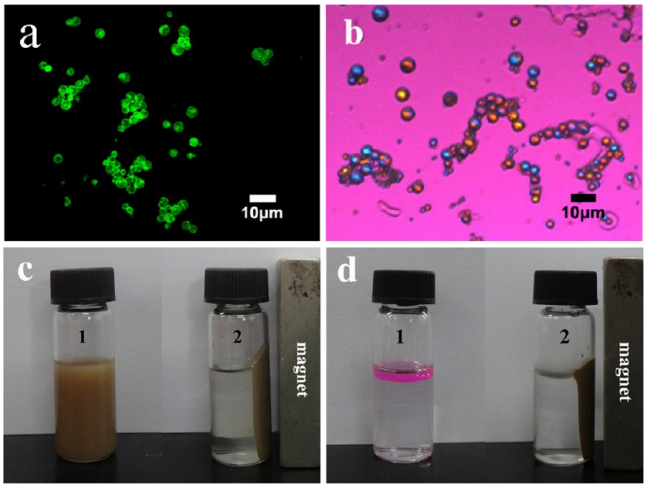

Figure 4. (a) Fluorescence microscopy image of the Janus composite cage (Figure 1a) after a preferential absorption of toluene, oil-soluble dye dil-C18 is added into toluene for easier observation. (b) Polarizing optical image of the Janus composite cage after a preferential absorption of paraffin wax inside the cavity. (c1) Paramagnetic Janus cage dispersed in water and (c2) after being collected with a magnet. (d1) Immiscible mixture of toluene (top)/water (bottom), oil-soluble dye dil-C18 is added in toluene. (d2) Manipulation of the oil contained paramagnetic Janus cage with a magnet.

about 2.1 g/g. The adsorption is completed fast within seconds. The fast adsorption may be related with the coarsened interior surface.[12] In order to further reveal location of oil in the cavity, a paraffin wax (T_m: 50–52 °C) is used. The polarizing optical microscopy image shows the paraffin crystallites are present inside the cage (Figure 4b). The paramagnetic Janus composite cage can move toward a magnet (Figure 4c). When the paramagnetic Janus composite cage is used, the oil absorbed cage can be manipulated using a magnet field (Figure 4d).

The Janus cages can be endowed responsive performance by grafting corresponding polymers, for example, a thermal responsive poly(*N*-isopropylacrylamide) (PNIPAM) with a lower critical solution temperature (LCST ~ 32 °C).[13] First, the parent inorganic Janus cage is prepared with amine and propenyl groups compartmentalized onto the exterior and interior surfaces of the shell (Figure 5a). The interior surface is smooth, and the exterior surface is coarsened (Figure 5b). There exist transverse channels across the shell. After the inorganic Janus cage is redispersed in water at 50 °C, the toluene solution of monomer NIPAM and initiator AIBN was favorably absorbed inside the cavity. At 70 °C, PNIPAM is

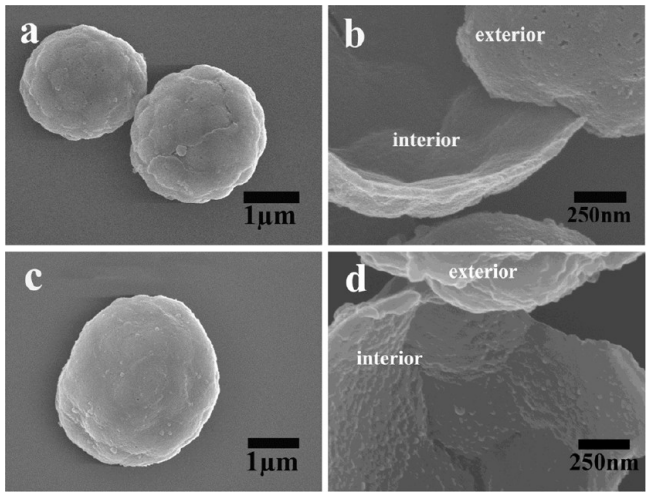

Figure 5. (a) SEM image of the parent inorganic Janus cage. (b) Exterior and interior surfaces of the inorganic Janus cage shell. (c) SEM image of the composite cage. (d) Interior surface of the composite cage.

grafted onto the interior surface, forming a thermally responsive Janus composite cage (Figure 5c). The interior surface becomes coarsened after grafting PNIPAM (Figure 5d). The characteristic peaks at 1544 and 1658 cm^{-1} are assigned to PNIPAM (Figure 6a). The Janus composite cage contains 53.6 wt % of PNIPAM measured by TGA in air (Figure 6b).

The Janus cage can collect toluene from their aqueous surroundings at high temperature, for example 50 °C (Figure 7a), due to the hydrophobic performance of the interior surface. Oil-soluble dye dil-C18 is added into toluene for easier observation under a fluorescence microscope. The Janus cage can collect toluene from their aqueous surroundings at high temperature, for example 50 °C, since the interior PNIPAM surface is hydrophobic above the lower critical solution temperature (LCST ~ 32 °C). The cavity of the Janus cage is filled with toluene after a preferential collection. As a result, the whole Janus cages demonstrate green under the fluorescence microscope (Figure 7a). When temperature decreases to 25 °C, the interior PNIPAM surface becomes hydrophilic below the LCST, and the collected toluene is rejected outwardly. As shown in Figure 7b, only a ring-shaped fluorescent green pattern is observed rather than the whole spherical green contour. The responsive Janus cages can provide a good microcontainer to favorably load desired materials and trigger release.

4. CONCLUSION

In summary, we have proposed a facile method to large scale produce polymer–inorganic bilayered composite Janus cages. They serve as robust micelle mimetic containers to selectively collect desired materials from their surroundings due to affinity difference. The cages are further functionalized by selectively growing responsive polymers by polymerization onto the interior surface, which is promising in controlled loading and release of desired materials. Paramagnetic Fe_3O_4 nanoparticles can be integrated within the composite shell; the Janus composite cages can be guided under a magnetic field.

dx.doi.org/10.1021/ma4006236 | *Macromolecules* 2013, 46, 4126–4130

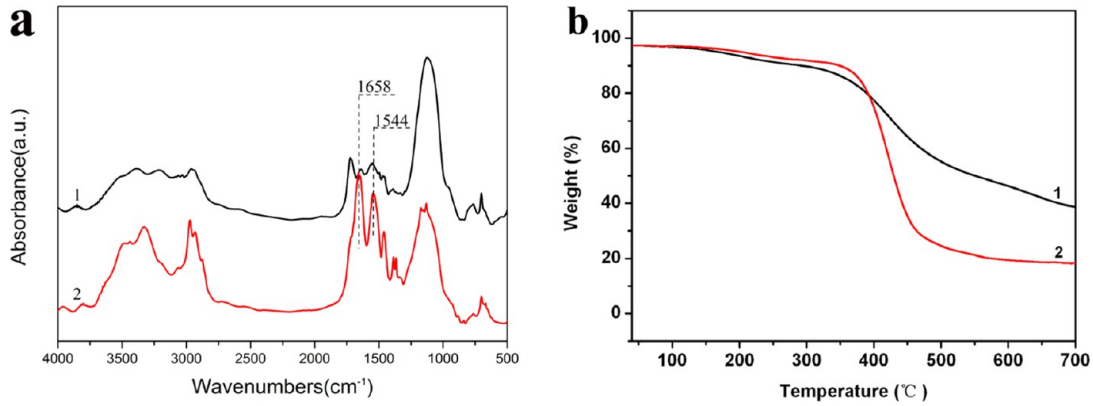

Figure 6. (a) FT-IR spectra and (b) thermogravimetric analysis (TGA) curves in air: (1) the as-synthesized parent inorganic Janus cage as shown in Figure 5a; (2) the PNIPAM–inorganic composite Janus cage as shown in Figure 5c.

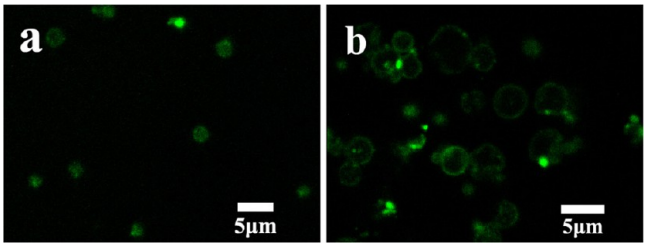

Figure 7. (a, b) Fluorescence microscopy images of the Janus composite cage after absorption of toluene at 50 and 25 °C, respectively. Oil-soluble dye dil-C18 is added into toluene for easier observation.

■ ASSOCIATED CONTENT

Supporting Information

Particle size and distribution, FT-IR spectrum, TGA curve, SEM and TEM images of silica cages and PDVB cages. This material is available free of charge via the Internet at http://pubs.acs.org.

■ AUTHOR INFORMATION

Corresponding Author

*E-mail: liangfuxin@iccas.ac.cn (F.L.); yangzz@iccas.ac.cn (Z.Y.).

Notes

The authors declare no competing financial interest.

■ ACKNOWLEDGMENTS

This work was supported by MOST (2012CB933200) and the NSF of China (51173191, 51233007, and 51173192).

■ REFERENCES

(1) de Gennes, P. G. *Rev. Mod. Phys.* **1992**, *64*, 645–648.
(2) (a) Perro, A.; Reculusa, S.; Ravaine, S.; Bourgeat-Lami, E.; Duguet, E. *J. Mater. Chem.* **2005**, *15*, 3745–3760. (b) Walther, A.; Müller, A. H. E. *Soft Matter* **2008**, *4*, 663–668. (c) Yang, S. M.; Kim, S. H.; Lim, J. M.; Yi, G. R. *J. Mater. Chem.* **2008**, *18*, 2177–2190. (d) Wang, C.; Xu, C.; Zeng, H.; Sun, S. *Adv. Mater.* **2009**, *21*, 3045–3052. (e) Wurm, F.; Kilbinger, A. F. M. *Angew. Chem., Int. Ed.* **2009**, *48*, 8412–8421. (f) Jiang, S.; Chen, Q.; Tripathy, M.; Luijten, E.; Schweizer, K. S.; Granick, S. *Adv. Mater.* **2010**, *22*, 1060–1071. (g) Lattuada, M.; Hatton, T. A. *Nano Today* **2011**, *6*, 286–308. (h) Walther, A.; Müller, A. H. E. *Chem. Rev.* **2013**, DOI: 10.1021/cr300089t.
(3) (a) Liu, B.; Wei, W.; Qu, X. Z.; Yang, Z. Z. *Angew. Chem., Int. Ed.* **2008**, *47*, 3973–3975. (b) Liu, B.; Zhang, C. L.; Liu, J. G.; Qu, X. Z.; Yang, Z. Z. *Chem. Commun.* **2009**, 3871–3873. (c) Zhang, C. L.; Liu, B.; Tang, C.; Liu, J. G.; Qu, X. Z.; Li, J. L.; Yang, Z. Z. *Chem. Commun.* **2010**, *46*, 4610–4612. (d) Tang, C.; Zhang, C. L.; Liu, J. G.; Qu, X. Z.; Li, J. L.; Yang, Z. Z. *Macromolecules* **2010**, *43*, 5114–5120.
(4) (a) MacCuspie, R. I.; Park, K.; Naik, R.; Vaia, R. A. *NSTI Nanotech* **2008**, *1*, 762–765. (b) Mair, L. O.; Evans, B.; Hall, A. R.; Carpenter, J.; Shields, A.; Ford, K.; Millard, M.; Superfine, R. *J. Phys. D: Appl. Phys.* **2011**, *44*, 125001. (c) Tan, L. H.; Xing, S. X.; Chen, T.; Chen, G.; Huang, X.; Zhang, H.; Chen, H. Y. *ACS Nano* **2009**, *3*, 3469–3474. (d) Chaudhary, K.; Chen, Q.; Juárez, J. J.; Granick, S.; Lewis, J. A. *J. Am. Chem. Soc.* **2012**, *134*, 12901–12903.
(5) (a) Liang, F. X.; Shen, K.; Qu, X. Z.; Zhang, C. L.; Wang, Q.; Li, J. L.; Liu, J. G.; Yang, Z. Z. *Angew. Chem., Int. Ed.* **2011**, *50*, 2379–2382. (b) Chen, Y.; Liang, F. X.; Yang, H. L.; Zhang, C. L.; Wang, Q.; Qu, X. Z.; Li, J. L.; Cai, Y. L.; Qiu, D.; Yang, Z. Z. *Macromolecules* **2012**, *45*, 1460–1467. (c) Walther, A.; Drechsler, M.; Müller, A. H. E. *Soft Matter* **2009**, *5*, 385–390. (d) Walther, A.; Andre, X.; Drechsler, M.; Abetz, V.; Müller, A. H. E. *J. Am. Chem. Soc.* **2007**, *129*, 6187–6198. (e) Bucaro, M. A.; Kolodner, P. R.; Taylor, J. A.; Sidorenko, A.; Aizenberg, J.; Krupenkin, T. N. *Langmuir* **2009**, *25*, 3876–3879.
(6) Liang, F. X.; Liu, J. G.; Zhang, C. L.; Qu, X. Z.; Li, J. L.; Yang, Z. Z. *Chem. Commun.* **2011**, *47*, 1231–1233.
(7) (a) Christian, D. A.; Tian, A. W.; Ellenbroek, W. G.; Levental, I.; Rajagopal, K.; Janmey, P. A.; Liu, A. J.; Baumgart, T.; Discher, D. E. *Nat. Mater.* **2009**, *8*, 843–849. (b) Meier, W. *Chem. Soc. Rev.* **2000**, *29*, 295–303. (c) McDonald, C. J.; Devon, M. J. *Adv. Colloid Interface Sci.* **2002**, *99*, 181–213. (d) Zeng, H. C. *J. Mater. Chem.* **2006**, *16*, 649–662. (e) Lou, X. W.; Wang, Y.; Yuan, C.; Lee, J. Y.; Archer, L. A. *Adv. Mater.* **2006**, *18*, 2325–2329. (f) Caruso, F. *Adv. Mater.* **2001**, *13*, 11–22.
(8) (a) Nakanishi, K.; Takahashi, R.; Nagakane, T.; Kitayama, K.; Koheiya, N.; Shikata, H.; Soga, N. *J. Sol-Gel Sci. Technol.* **2000**, *17*, 191–210. (b) Kamio, E.; Yonemura, S.; Ono, T.; Yoshizawa, H. *Langmuir* **2008**, *24*, 13287–13298.
(9) Jin, Z. G.; Wang, Y. D.; Liu, J. G.; Yang, Z. Z. *Polymer* **2008**, *49*, 2903–2910.
(10) Li, G. Z.; Peng, W. C.; Li, X. Y.; Fan, X. B.; Li, X. J.; Zhang, G. L.; Zhang, F. B. *Appl. Surf. Sci.* **2008**, *254*, 4970–4979.
(11) Brinker, C. J.; Scherer, G. W. *Sol-Gel Science: The Physics and Chemistry of Sol-Gel Processing*; Academic Press: San Diego, CA, 1990; Chapter 3, pp 99–127.
(12) (a) Feng, L.; Li, S. H.; Li, Y. S.; Li, H. J.; Zhang, L. J.; Zhai, J.; Song, Y. L.; Liu, B. Q.; Jiang, L.; Zhu, D. B. *Adv. Mater.* **2002**, *14*, 1857–1860. (b) Wang, Q.; Li, J. L.; Zhang, C. L.; Qu, X. Z.; Liu, J. G.; Yang, Z. Z. *J. Mater. Chem.* **2010**, *20*, 3211–3215.
(13) (a) Otake, K.; Inomata, H.; Konno, M.; Saito, S. *Macromolecules* **1990**, *23*, 283–289. (b) Wang, X. H.; Qiu, X. P.; Wu, C. *Macromolecules* **1998**, *31*, 2972–2976.